

STEREO EVALUATION OF CARTOSAT-1 DATA SUMMARY OF DLR RESULTS DURING CARTOSAT-1 SCIENTIFIC ASSESSMENT PROGRAM

Manfred Lehner, Pablo d'Angelo, Rupert Müller, Peter Reinartz

German Aerospace Center (DLR), Remote Sensing Technology Institute, Oberpfaffenhofen, 82234 Wessling,
Germany

{Manfred.Lehner, Pablo.Angelo, Rupert.Mueller, Peter.Reinartz}@dlr.de

Commission I, SS-11

KEY WORDS: CARTOSAT-1, Stereoscopic CCD scanner, Rational polynomial model, Matching, DSM generation, Orthoimage, Accuracy analysis

ABSTRACT:

The Remote Sensing Technology Institute (IMF) of the German Aerospace Center (DLR) has more than 20 years of history in developing spaceborne stereo scanners and the corresponding stereo evaluation software systems. It takes part in the CARTOSAT-1 Scientific Assessment Program (C-SAP) as a principal investigator for German (Southeast Bavaria) and Spanish (Catalonia) test sites and as a Co-I for a French test site (Mausanne-les-Alpilles). A rich variety of landscapes is present in these three test sites. In all cases ground truth in form of GCP (or orthoimages of high resolution) and DTM/DSM (digital terrain or surface models) of sufficient accuracy have been delivered by the principal investigators. Rational polynomial functions (RPC) are provided by the distributing Indian agency (Space Applications Centre (SAC) of ISRO, Ahmedabad) as a universal sensor model for each scene. The inherent absolute orientation accuracy of the RPC models in the CARTOSAT-1 stereo imagery used here turned out to be around 100 m (normally). Thus, to exploit the high resolution of 2.5 m, RPC have to be corrected via the available ground truth. It is shown that the correction by an affine transformation is necessary in order to achieve sub-pixel accuracy in the stereo evaluation of full scenes. The remaining standard deviations of the residuals in image space during RPC correction are about 0.5-1 pixel in ground control points (GCP). Stereo evaluation is done by DLR processing software. Hierarchical intensity based matching and subsequent region growing are used to automatically derive a dense set of stereo tie points. An effective blunder reduction is based upon bi-directional LSM, quasi-epipolar reprojection of the tie points, and control of residuals in stereo forward intersection. Shifts between aft/fore orthoimages are found to be in sub-pixel range. DSM accuracy assessment is done via the statistics of height differences compiled by the forward intersection software. This is sufficient if accurate GCP for RPC correction are available. For direct comparison of the generated DSM with the reference DTM/DSM a 3D shift is estimated via least squares adjustment and mean and standard deviations of the DTM/DSM differences after shifting are provided. In summary, standard deviations of 2-4 m are achieved.

1. INTRODUCTION

1.1 DLR participation in C-SAP

DLR is engaged in 3-line stereo scanner development and data evaluation since 1980 when ISRO offered to fly such a DLR camera on SROSS-I satellite to be launched by Indian ASLV rocket in 1988. The camera has been built and the German photogrammetric community and also ISRO/SAC could exploit airborne 3-line scanner imagery of a MEOSS camera model from 1986 onwards (Lehner and Gill 1992, Heipke et al. 1996). DLR in subsequent years concentrated on the German 3-line scanner MOMS-02 which was successfully flown as MOMS-02/D2 instrument on space shuttle mission D2 in 1993 and as MOMS-2P on the Russian space station Mir from 1996 till 1999. MOMS mission brought the development of a MOMS stereo work station at DLR through cooperation of DLR with several German universities (Seige et al. 1998, Kornus et al. 2000).

The next along-track stereo scanner in space investigated at DLR/MF was the HRS instrument on SPOT-5 (launched in May 2002). DLR took part as a PI in the HRS scientific assessment program in 2003-2004 (Reinartz et al. 2006).

In the following years the DLR stereo evaluation and ortho-projection software which was up to then based on rigorous modelling only was supplemented by software for RPC based ortho-projection, forward intersection, RPC correction, and quasi-epipolar reprojection of stereo pairs. This was necessary for the orthoimage and DSM generation from the new high resolution monoscopic and stereo imagery of IKONOS-2 and QuickBird satellites (Lehner et al. 2005).

In May 2005 India launched its IRS-P5 satellite with CARTOSAT-1 instrument which is a dual-optics 2-line along-track stereoscopic pushbroom scanner with the very interesting resolution of 2.5 m which is adequate for many 3D mapping tasks. The operational use of the data is described in (Srivastava et al. 2007). After approximately one year of operation for the 3D mapping of India, from June 2006 onwards data were made available to international investigators in the frame of the CARTOSAT-1 Scientific Assessment Program (C-SAP) by the Space Applications Centre (SAC, Ahmedabad) of the Indian Space Research Organisation (ISRO). Intermediate results have been presented by PI and Co-I during ISPRS TC IV symposium in Goa (India) in September 2006 and during ISPRS Inter-Commission workshop in Hanover (Germany) in May/June 2007.

A final report on the DLR/IMF results achieved for CSAP together with a set of DSM and orthoimages has been delivered to ISRO/SAC. A copy of the report can be provided to interested readers.

1.2 DLR test sites for CSAP

DLR/IMF takes part in CARTOSAT-1 Scientific Assessment Program (C-SAP) as a principal investigator for German (Southeast Bavaria) and Spanish (Catalonia, test site 10) test sites, and as a Co-I in the evaluation of CARTOSAT-1 data for test site 5 (Mausanne-les-Alpilles, France). In all cases rational polynomial functions (RPC) are provided by the distributing Indian agency ISRO/SAC as a universal sensor model for each scene. Table 1 shows the imaging dates and the centre roll angle which is varying substantially (e.g. for Mausanne scenes for producing the overlap).

| Abbreviation for the paper for aft and fore scenes | Imaging date | Centre-roll (deg) (for aft image) |
|--|--------------|-----------------------------------|
| Mausanne-les-Alpilles (France), test site 5 | | |
| MA1 / MF1 | 31Jan2006 | -13.6 |
| MA2 / MF2 | 06Feb2006 | 4.0 |
| Catalonia (Spain), test site 10 | | |
| Cat-A / Cat-F | 01Feb2006 | -0.1 |
| Bavaria (Germany) | | |
| Bav-A / Bav-F | 30Apr2007 | 9.5 |

Table 1: The 4 stereo pairs used for C-SAP at DLR

Some numbers in the tables given in this paper may be slightly different from those in (Lehner et al. 2006/2007) because the original RPC delivered with the images had zero denominator problems and were later replaced with new RPC by ISRO/SAC.

2. DLR STEREO PROCESSING

2.1 Image matching

Hierarchical intensity based matching as implemented into the XDibias image processing system of DLR/IMF consists of two major steps (Lehner and Gill 1992; Kornus et al. 2000). In a first step the matching process uses a resolution pyramid to cope even with large stereo image distortions stemming from carrier movement and terrain. Large local parallaxes can be handled without knowledge of exterior orientation (which is often not available with sufficient accuracy for space-borne imagery). The selection of pattern windows is based on the Foerstner interest operator which is applied to one of the stereo partners (chosen according to the best radiometric properties – in case of CARTOSAT-1 this is the aft image). For selection of search areas in the other stereo partner(s) local affine transformations are estimated based on already available tie points in the neighborhood (normally from a coarser level of the image pyramid; on the coarsest level (factor 64 reduction in case of CARTOSAT-1 stereo pairs) the parallaxes and shifts are already so small that the process can be started automatically just using adapted (larger) window sizes for patterns and search areas). Tie points with an accuracy of one pixel are located via the maximum of the normalized correlation coefficients computed by sliding the pattern area all over the search area.

These approximate tie point coordinates are refined to sub-pixel accuracy by local least squares matching (LSM). The number of points found and their final (sub-pixel) accuracy achieved depend mainly on image similarity and decrease with increasing stereo angles or time gaps between imaging. The software was originally devised for along-track 3-line stereo imaging (stereo scanners MEOSS and MOMS operated by DLR). Normally, the procedure can be executed fully automatically if the shift between the stereo partners is small compared to the image size as is true for CARTOSAT-1 stereo pairs. The procedure results in a rather sparse set of tie points well suited for introducing them into bundle adjustment and as an excellent source of seed points for further densification via region growing (second step).

The second step uses the region growing concept first published by Otto and Chau in the implementation of TU Munich (Heipke et al. 1996). It combines LSM with a strategy for local propagation of initial conditions of LSM.

Various methods for blunder reduction are used for both steps of the matching:

- Threshold for correlation coefficient
- Bi-directional matching and threshold on resulting shifts of the coordinates
- Quasi-epipolar reprojection of tie point coordinates

In areas of low contrast the propagation of affine transformation parameters for LSM in the region growing process leads to high rates of blunders. In order to avoid intrusion into homogeneous image areas (e.g. roof planes and agricultural fields without structure) the extracted image chips are subject to (low) thresholds on variance and roundness of the Foerstner interest operator. This and the many occlusions found in densely built-up areas imaged with a large stereo angle create lots of insurmountable barriers for region growing. Thus, for high resolution stereo imagery the massive number of seed points provided by the matching in step one (image pyramid) turns out to be essential for the success of the region growing.

The numbers of tie points found and their sub-pixel accuracy is highly dependent on the stereo angle. A large stereo angle (large base to height ratio b/h) leads to poorer numbers of tie points and to lower accuracy in LSM via increasing dissimilarity of the (correctly) extracted image chips.

For currently available high resolution stereo imagery the stereo angle is too large, at least for built-up areas. The importance of a large base-to-height ratio is exaggerated at the cost of the matching accuracy and density (see Krauss et al. 2006). The accuracy in forward intersection is inversely proportional to the base-to-height ratio but also direct proportional to the matching accuracy (parallax measurement). The latter and the matching density are improved by reducing the stereo angle. In table 2 past and current stereo missions are shown together with their stereo angles. In contrast to the drastic reduction in ground sampling distance (GSD) the stereo angles are growing instead of decreasing. Thus, image matching performance is much hindered because of the appearance of more and more complex natural and man-made objects in the images. For IKONOS-2 the possibility for smaller stereo angles exists. As indicated in the table 2 DLR managed to get examples with 10 and 6 degree stereo angles and the advantage for image matching could be shown (Krauss et al. 2006). An increase in the accuracy of the parallax measurement via finer resolution allows for a decrease of the stereo angle to improve matching performance.

| Sensor | GSD (m) | Stereo angle (degree) |
|--------------|---------|------------------------|
| MOMS-2P | 18 | (2 x) 21.45 |
| SPOT-5 HRS | 10/5 | 40 |
| ALOS / PRISM | 2.5 | (2 x) 23.8 |
| CARTOSAT-1 | 2.5 | 31 |
| IKONOS-2 | 1 | ~30 (Special: 10/6) |
| QuickBird | 0.6 | ~60 |

Table 2: Stereo angles and stereo missions

2.2 RPC correction

In (Lehner et al. 2006) it is shown for the stereo pair M1A/F that for a full scene a pure bias correction of RPC results in residuals which are not acceptable: larger than 1 pixel and with systematic behaviour. Since then better GCP could be retrieved for all stereo pairs. By their use this finding can be consolidated: for full CARTOSAT-1 stereo pairs the correction of the provider supplied RPC via an affine transformation is necessary to achieve sub-pixel accuracy. Table 3 gives the summary of bias versus affine correction for all the stereo pairs used at DLR for CSAP.

| Image | Number of GCP | Standard deviation of residuals after | | | |
|------------------|---------------|---------------------------------------|--------|-------------------|--------|
| | | bias correction | | affine correction | |
| | | row | column | row | column |
| Cat-A | 70 | 0.74 | 0.58 | 0.51 | 0.41 |
| Cat-F | 68 | 1.64 | 0.53 | 0.56 | 0.44 |
| M1A | 31 | 1.39 | 3.38 | 0.76 | 0.56 |
| M1F | 30 | 2.38 | 4.46 | 0.73 | 0.68 |
| M2A | 9 | 1.12 | 1.46 | 0.43 | 0.45 |
| M2F | 9 | 1.59 | 1.20 | 0.34 | 0.33 |
| Bav-AT | 14 | 0.48 | 0.56 | 0.35 | 0.53 |
| Bav-FT | 14 | 0.80 | 0.64 | 0.64 | 0.62 |
| Bav-A full scene | 30 | 1.17 | 0.60 | 0.50 | 0.54 |

Table 3: Standard deviations of residuals at GCP after bias and affine correction of RPC for various CARTOSAT-1 stereo pairs

For smaller parts of the images as for the Bavarian Taching test area (GCP only in this area indicated by the image names Bav-AT/FT – this is about 1/9th of a full scene) a bias correction may lead to acceptable results for this sub-area. In order to illustrate the nature of the residuals for bias and affine RPC correction the shifts are plotted in figures 1 and 2 for the Catalonian case with the large number of accurate GCP. It can be seen that the pattern of the residuals in the bias case is rather complex and can not even be handled by just an additional rotation. In contrast, the residuals in figure 2 from the correction with an affine transformation do not show any systematic behaviour. Of course, if only an inadequate distribution of GCP is available it may be worse to do affine instead of bias correction. A well distributed set of GCP of high accuracy is needed for an optimal result.

In (Lehner et al. 2007) it has been reported already that forward intersection results are often poor without RPC correction (too large residuals in image space).

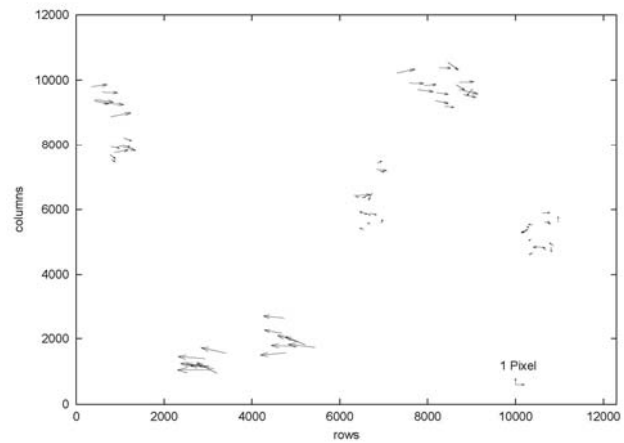


Figure 1: Residual vectors from bias correction for the 68 GCP for Cat-F

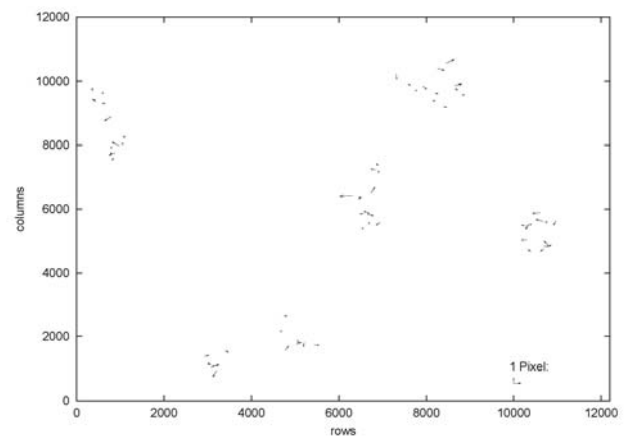


Figure 2: Residual vectors from affine transformation correction for the 68 GCP for Cat-F

2.3 RPC forward intersection

Forward intersection is done via iterative least squares adjustment using $2n$ (for n stereo partners) observation equations (Grodecki et al. 2004, Lehner et al. 2006). Normally, in this report on CARTOSAT-1 n is 2 and 4 equations are established per stereo tie point for the derivation of the 3 object space coordinates longitude, latitude and ellipsoidal height in WGS84 datum. The initial values for the object space coordinates longitude and latitude are derived from an affine transformation using the corner coordinates given by the image provider. Initial height values are taken from a DTM (or, alternatively, the mean height of the area under investigation can be used – this is not critical for the convergence). Normally, convergence is achieved after 2 iterations. If a DTM/DSM is given as an additional input a statistic of the differences of the generated heights and the reference DTM/DSM heights is established.

The residuals in image space can be used for blunder detection. Of course, only residuals in cross track direction will be effective because wrong row coordinates of tie points are translated into wrong height values if only two stereo partners

are available (stereo imaging direction). A threshold of 0.5 pixel is used throughout this report for acceptance of forward intersection results.

2.4 Blunder reduction

Blunder reduction is done during and after image matching and during forward intersection. Most of the methods for image matching are mentioned in section 3.1. Additionally, some blunders can be detected via quasi-epipolar reprojection of the stereo pair. For this best points from hierarchical matching are used to estimate an affine transformation from fore to aft CARTOSAT image. The standard deviation σ for the column residuals of this affine transformation is very small ($\sigma = 0.2-0.3$ pixel). The fore coordinate pairs of the mass stereo tie points are transformed with this affine transformation. All points are rejected for which the absolute value of the difference of the column coordinates of the aft tie points and the transformed fore tie points is larger than the threshold 3σ . This blunder check is not independent of the blunder check via the residuals in image space during forward intersection.

2.5 DSM interpolation and orthoimage generation

A regular DSM is generated from the point clouds produced by forward intersection via triangulation and interpolation (Hoja et al. 2005). DSM editing via cloud- and water-masks etc. is under investigation, as well as DSM fusion for separately produced CARTOSAT-1 DSM and existing DSM from other sources.

After derivation of the DSM orthoimages with user defined datum and projection can be generated using the affine corrected RPC and the DSM. Accuracy evaluations based on orthoimage comparison of aft and fore sensor are given in (Lehner et al. 2007) with more details.

3. RESULTS FOR THE DIFFERENT TEST SITES

3.1 Catalonia

A reference DTM with a GSD of 15 m (height accuracy 1.1 m) and 10 orthoimages with a resolution of 0.5 m are provided by the Institut Cartogràfic de Catalunya (ICC). 70 GCP have been measured in the orthoimages and the stereo partner Cat-A with sub-pixel precision. These measurements have been automatically transformed into Cat-A/F tie points via least squares matching using mass points from hierarchical matching for initial guesses of Cat-F coordinates and least squares matching (LSM) with several window sizes. Thus, 68 GCP for Cat-F could be derived – well fitting to the Cat-A GCP in terms of stereo tie points. 6 window sizes from 17 to 27 have been used in LSM in order to get statistical values for the accuracy. The mean standard deviations in rows and columns for the 68 GCP and 6 window sizes were below 0.1 pixel. Consistent stereo tie points are derived by this procedure.

The standard deviations of the residuals in RPC correction are given in table 3 and a plot of the residual vectors for the fore image is provided in figure 2. The shift parts of the affine transformations for RPC correction are given in table 4 for all stereo pairs, normally (besides M1A/F) corresponding well with the expected orbit/attitude accuracy of a few hundred meters (better than 160 m along-track and 100 m across-track).

After RPC correction the DSM is derived through image matching and forward intersection. A few numbers for illustrating the results are given in table 5. For each stereo pair the number of matches passing through forward intersection (using the threshold of 0.5 pixel for all 4 residuals in image space) is given for the best tie points from hierarchical matching (HM) and for all points after region growing (RG). Additionally, the mean height difference and the standard deviation of the height differences to the reference DSM/DTM are provided. There is no distinction on land use. Thus, for the small Taching area with a high percentage of forests with tall trees this gives a wrong picture which will be put right to some extent in the section 3.3 on Bavaria.

| Image | Number of GCP | Shift part of affine transformation (pixel) | |
|--------|---------------|---|---------|
| | | row | column |
| Cat-A | 70 | -32.66 | -16.95 |
| Cat-F | 68 | -48.42 | 1.47 |
| M1A | 31 | -2231.59 | -685.14 |
| M1F | 30 | -2335.86 | -546.46 |
| M2A | 9 | -40.08 | -6.01 |
| M2F | 9 | -50.83 | -0.56 |
| Bav-AT | 14 | 52.38 | -8.60 |
| Bav-FT | 14 | 62.07 | 38.18 |

Table 4: Shift parts of the affine transformations for RPC correction for visualization of absolute positional accuracy of original RPC

| Stereo pair / matching step | Number of accepted tie points (million) | Height difference: reference DTM/DSM minus Cartosat-DSM (m) | |
|-----------------------------|---|---|----------|
| | | mean | σ |
| Cat / HM | 0.06 | -0.6 | 1.83 |
| Cat / RG | 7.08 | -1.0 | 3.05 |
| M1 / HM | 0.01 | -1.9 | 2.24 |
| M1 / RG | 4.82 | -1.4 | 3.80 |
| M2 / HM | 0.03 | -1.5 | 2.21 |
| M2 / RG | 6.14 | -1.1 | 3.53 |
| Bav / HG-T | 0.006 | -3.6 | 4.18 |
| Bav / RG-T | 1.09 | -3.6 | 7.29 |

Table 5: Number of tie points accepted during forward intersection for 2 matching steps (HM: excellent points from hierarchical matching / RG: all points from region growing) and mean and standard deviation of height differences to the reference DSM (M1/2) or DTM (Cat and Bav, T: Taching area only)

Orthoimages Cat-A-ortho and Cat-F-ortho are computed based on corrected RPC and the DSM produced via triangulation and interpolation from the accepted matches from region growing. The matching between Cat-A/F-ortho gives shift vectors with a mean of (0.10, 0.06) and a standard deviation of (0.16, 0.24) for rows and columns, respectively (in pixel, about 45000 tie points excluding the coast area are used). Thus, in regions of acceptable density of matches, i.e. in areas where the DSM interpolation has enough support, the fit between the orthoimages is very satisfactory.

3.2 Mausanne-les-Alpilles

Two stereo scenes are available for this area with an overlap of nearly half a scene. Thus, there was a chance for separate and common evaluations. GCP from a GPS campaign were provided by the principal investigator from the Joint Research Centre of the European Commission (JRC, Institute for the Protection and Security of the Citizen, Agriculture and Fisheries Unit) for stereo pair M1. Via several matching steps 9 of these GCP could be transferred to stereo pair M2 (in the overlap region). The RPC correction summary is given in table 3, the summary of the separate DSM processing in table 5.

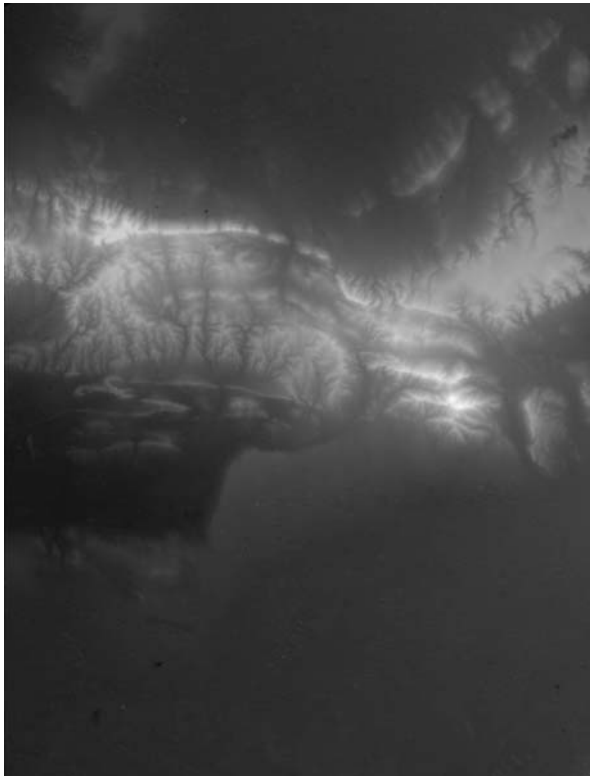


Figure 3: DSM in overlap area of stereo pairs M1/2 (grid spacing 10 m, size of area 17.9 km x 23.5 km)

The orthoimage check matching was made for the stereo pair M1. The about 23400 shift vectors have a mean of (0.11, 0.21) and a standard deviation of (0.18, 0.32) for rows and columns, respectively.

Special processing of the overlap area of M1/M2:

In order to derive 4-ray tie points the matching for the overlap area was done through the following steps:

1. hierarchical matching of overlap regions of the aft images (M1A and M2A)
2. region growing for densification
3. transfer of matched points to the corresponding fore images (M1A to M1F and M2A to M2F) by a special transfer point matching feature of the region growing software

The numbers of points accepted in multi-ray forward intersection is given in table 6 together with the number achieved when merging the object space points found in the separate processing of the stereo pairs M1 and M2 (last row of

table 6). The latter number is much larger than the number of 4-ray points. This can be attributed to difficulties of multi-temporal and multi-direction matching. Also the cloud region available in the overlap area is of course fully missing in the 4-ray tie point set which is a further disadvantage. The standard deviations of the height differences are comparable.

| Matching partners | Rays | Nr. of accepted tie points (million) | Height difference: reference DSM minus Cartosat-DSM (m) | |
|---------------------------|------|--------------------------------------|---|----------|
| | | | mean | σ |
| from forward intersection | | | | |
| M1A/M2A | 2 | 4.60 | -2.1 | 5.51 |
| M1A/M2A /M1F | 3 | 2.13 | -1.4 | 3.64 |
| M1A/M2A /M1F/M2F | 4 | 1.22 | -1.3 | 3.36 |
| DSM/DSM shift estimation | | | | |
| M1A/F | 2 | 2.16 | -0.77 | 3.2 |
| M2A/F | | 2.23 | | |

Table 6: Matching experiment in the overlap region of the 2 Mausanne stereo pairs

Thus, the pure merging of the separate matching and forward intersection results is more promising for practical purposes. The lateral shift vector of this 4.39 million point set versus the reference DSM is (3.2 m, -3.1 m). Figure 3 shows the DSM derived by merging of the point sets for the overlap area.

3.3 Bavaria

A laser DTM of the Bavarian Survey for the Taching area is available (5 km x 5 km, 5 m grid spacing). For GCP extraction an orthoimage of 2 m GSD could be retrieved from the Geoweb server of the Bavarian Survey (figure 5). 14 GCP are extracted from orthoimage and Bav-A and complemented to stereo tie points via LSM (as described for Catalonia). Evaluations reported here are restricted to this small Taching subset of the Bavarian stereo pair (see table 3 for RPC correction results). The results in table 5 show a large standard deviation of the height differences to the reference DTM. In order to prove the influence of the forest parts the laser DTM was subtracted from the (smoothed) Cartosat-DSM. In the difference image all pixels with values larger than 10 m are marked black. The result is shown in figure 4. A good correspondence of the black areas with the forest areas in figure 5 (orthoimage of Bavarian Survey) exists. This explains the high standard deviations in table 5.

4. CONCLUSIONS

Comparisons of the generated DSM with the JRC and ICC reference DSM/DTM result in standard deviations of the height differences of 3-4 meters after affine correction of RPC (for full scenes / case Bavaria excluded). This should be ranked as a very good result because no object classification in terms of DSM/DTM differences is applied. Thus, CARTOSAT-1 stereo imagery is well suited for the derivation of DSM and orthoimages with 1-2 pixel vertical accuracy (1 σ) in terrain with good pattern matching characteristics and moderate slope angles. Prerequisite to achieve this accuracy is a set of well distributed GCP of high accuracy for RPC correction (about half pixel standard deviation at GCP). In mountainous terrain

and with rather low sun elevations the normal problems of too steep slopes and large shadow areas without enough matching targets lead to local artefacts in the DSM generated from 2-fold stereo imagery with the software described here.

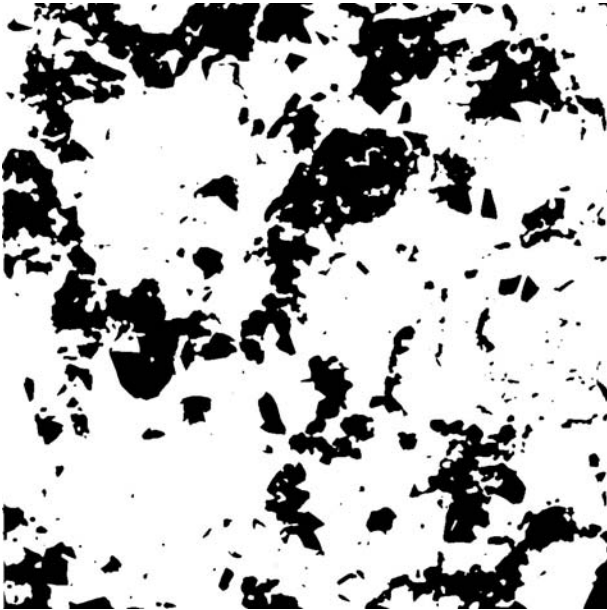


Figure 4: Differences from DSM derived from CARTOSAT stereo pair and laser DTM from Bavarian Survey larger than 10 m are marked in black – a good correlation with forest areas in the orthoimage (figure 5) shows up



Figure 5: Orthoimage of Taching area from Bavarian Survey as a source for GCP (2 m sampling)

ACKNOWLEDGEMENTS

The big effort by ISRO/SAC of offering a CARTOSAT-1 Scientific Assessment Program to the ISPRS community is much appreciated. Acknowledgements also go to the JRC scientists for the preparation of valuable ground truth for test site 5 and to the Institut Cartographic de Catalunya for the delivery of adequate ground truth for test site 10.

REFERENCES

Grodecki, J., Dial, G., Lutes, J., 2004: Mathematical Model for 3D feature extraction from multiple satellite images described by RPCs, ASPRS Annual Conf. Proc., Denver, Colorado, USA

Heipke, C., Kornus, W., Pfannenstien, A., 1996: The evaluation of MEOS airborne 3-line scanner imagery – processing chain and results, Photogrammetric Engineering and Remote Sensing, Vol. 62, No. 3, pp. 293-299

Hoja, D., Reinartz, P., Lehner, M., 2005: DSM Generation from High Resolution Satellite Imagery Using Additional Information Contained in Existing DSM, Proc. of the ISPRS Workshop 2005 High Resolution Imaging for Geospatial Information, Hanover, Germany

Kornus W., Lehner M., Schroeder, M., 2000: Geometric inflight calibration by block adjustment using MOMS-2P 3-line-imagery of three intersecting stereo-strips, SFPT (Société Française de Photogrammétrie et Télédétection) , Bulletin Nr. 159, pp. 42-54

Krauss T., Lehner M., Reinartz P., Stilla U., 2006: Comparison of DSM Generation Methods on IKONOS Images, Photogrammetrie-Fernerkundung-Geoinformation Nr. 4, pp. 303-314

Lehner M., Gill, R.S., 1992: Semi-Automatic Derivation of Digital Elevation Models from Stereoscopic 3-Line Scanner Data, *IAPRS*, Vol. 29, part B4, Commission IV, pp. 68-75, Washington, USA

Lehner, M., Müller, Rupert, Reinartz, P., 2005: DSM and Orthoimages from QuickBird and Ikonos Data Using Rational Polynomial Functions, Proc. of High Resolution Earth Imaging for Geospatial Information, May 17-20, Hanover, Germany

Lehner, M., Müller, Rupert, Reinartz, P., 2006: Stereo Evaluation of CARTOSAT-1 Data on Test Site 5 – First DLR Results, Proc. of ISPRS-TC IV Symposium, Sept. 27-30, Goa, India

Lehner, M., Müller, Rupert, Reinartz, P., Schroeder, M., 2007: Stereo evaluation of Cartosat-1 data for French and Catalanian test sites, Proc. of the ISPRS Workshop 2007 High Resolution Earth Imaging for Geospatial Information, Hanover, Germany, May 29 – June 1

Reinartz, P., Müller, Rupert, Lehner, M., Schroeder, M., 2006: Accuracy Analysis for DSM and orthoimages derived from SPOT HRS stereo data using direct georeferencing, *ISPRS Journal of Photogrammetry & Remote Sensing* 60, pp. 160-169

Seige, P., Reinartz, P., Schroeder, M., 1998: The MOMS-2P mission on the MIR station, *IAPRS*, Vol. 32, Part 1, pp. 204-210, Bangalore, India (see also <http://www.nz.dlr.de/moms2p>)

Srivastava P.K., Srinivasan T.P., Gupta Amit, Singh Sanjay, Nain J.S., Amitabh, Prakash S., Kartikeyan B., Gopala Krishna B., 2007: Recent Advances in CARTOSAT-1 Data Processing, Proc. of the ISPRS Workshop on High Resolution Earth Imaging for Geospatial Information, Hanover, Germany, May 29 – June 1